HHS Public Access

Author manuscript

Oncogene. Author manuscript; available in PMC 2017 August 14.

Published in final edited form as:

Oncogene. 2016 May 19; 35(20): 2645–2654. doi:10.1038/onc.2015.327.

Mice deficient in Muc4 are resistant to experimental colitis and colitis-associated colorectal cancer

S Das[1,7], **S Rachagani**[1], **Y Sheinin**[2], **LM Smith**[3], **CB Gurumurthy**[4], **HK Roy**[5], and **SK Batra**[1,6]

[1]Department of Biochemistry and Molecular Biology, University of Nebraska Medical Center, Omaha, NE, USA

[2]Department of Pathology, University of Nebraska Medical Center, Omaha, NE, USA

[3]Department of Biostatistics, University of Nebraska Medical Center, Omaha, NE, USA

[4]Mouse Genome Engineering Core Facility, Department of Genetics, Cell Biology and Anatomy, University of Nebraska Medical Center, Omaha, NE, USA

[5]Center for Digestive Disorders, Boston University School of Medicine, Boston, MA, USA

[6]Buffett Cancer Center, Eppley Institute for Research in Cancer and Allied Diseases, University of Nebraska Medical Center, Omaha, NE, USA

Abstract

MUC4, a large transmembrane mucin normally expressed in the small and large intestine, is differentially expressed during inflammatory and malignant conditions of the colon. However, the expression pattern and the role of MUC4 in colitis and colorectal cancer (CRC) are inconclusive. Therefore, the aim of this study was to understand the role of Muc4 during inflammatory and malignant conditions of the colon. Here, we generated *Muc4*$^{-/-}$ mice and addressed its role in colitis and colitis-associated CRC using dextran sodium sulfate (DSS) and azoxymethane (AOM)-DSS experimental models, respectively. *Muc4*$^{-/-}$ mice were viable, fertile with no apparent defects. *Muc4*$^{-/-}$ mice displayed increased resistance to DSS-induced colitis compared with wild-type (WT) littermates that was evaluated by survival rate, body weight loss, diarrhea and fecal blood score, and histological score. Reduced infiltration of inflammatory cells, that is, CD3^{+} lymphocytes and F4/80^{+} macrophages was observed in the inflamed mucosa along with reduction in the mRNA levels of inflammatory cytokines interleukin (*IL*)-*1β* and tumor necrosis factor *(TNF)-α* and anti-microbial genes *Lysozyme M* and *SLPI* in the colon of *Muc4*$^{-/-}$ mice compared with WT littermates. Compensatory upregulation of *Muc2* and *Muc3* mucins under basal and DSS treatment conditions partly explains the resistance observed in *Muc4*$^{-/-}$ mice. Accordingly,

Correspondence: Dr SK Batra, Department of Biochemistry and Molecular Biology, Buffett Cancer Center, Eppley Institute for Research in Cancer and Allied Diseases, University of Nebraska Medical Center, Omaha, NE 68198-5870, USA. sbatra@unmc.edu.
[7]Current Address: Department of Medicine, Karolinska Universitetssjukhuset, Solna, Stockholm 171 76, Sweden.

CONFLICT OF INTEREST

The authors declare no conflict of interest.

AUTHOR CONTRIBUTIONS

SD, SR and SKB: study concept and design; SD and SR: acquisition of data; CBG: generation of *Muc4*$^{-/-}$ mice; YS: histopathological analysis; LMS: statistics; SD, SR, HKR and SKB: analysis and interpretation of data; SD and SKB: wrote the manuscript.

Supplementary Information accompanies this paper on the Oncogene website (http://www.nature.com/onc)

Muc4$^{-/-}$ mice exhibited significantly reduced tumor burden compared with WT mice assessed in a colitis-induced tumor model using AOM/DSS. An increased percentage of Ki67^{+} nuclei was observed in the tumors from WT compared with *Muc4*$^{-/-}$ mice suggesting Muc4 to be critical in intestinal cell proliferation during tumorigenesis. Taken together, we conclusively demonstrate for the first time the role of Muc4 in driving intestinal inflammation and inflammation-associated tumorigenesis using a novel *Muc4*$^{-/-}$ mouse model.

INTRODUCTION

Colorectal cancer (CRC) is the third most commonly diagnosed and lethal cancer in the United States.[1] Inflammatory conditions in the gastrointestinal tract referred to as inflammatory bowel disease (IBD) that includes ulcerative colitis (UC) and Crohn's disease (CD) pose a significant risk for the development of CRC.[2] Although the etiology of IBD is complex with multiple genetic and environmental factors, dysregulation in intestinal mucus barrier constitutes an important etiological factor.[2]

The gastrointestinal system is remarkable with respect to the organization of protective mucus barrier, where the secretory mucins form the outer loose and inner dense layer and the membrane-bound mucins form the glycocalyx that covers and protects the surface epithelial cells.[3] MUC2 is the principal secretory mucin in both the small and large intestine.[3] The transmembrane mucins that comprise the glycocalyx on the surface of intestinal epithelial cells include MUC1, MUC3, MUC4, MUC12, MUC13 and MUC17.[3] In humans, MUC1 is expressed at low levels in both small and large intestine, MUC3 predominantly expressed in small intestine[4] and MUC4 is found in equivalent amounts in both small and large intestine.[5] This normal distribution of mucins in the mucus layer changes during infection and intestinal inflammatory conditions such as UC and CD.[2] Several studies have looked into the expression pattern of different mucins in patient samples with inconclusive findings.[2,6–9] The discrepancies observed could be due to several reasons: stage of the disease tissues collected, antibodies used, glycosylation status of the mucins and so on. To address the role of mucins in intestinal health and disease, knockout mouse models of Muc1,[10] Muc2(ref. 11) and Muc13(ref. 12) have been used. Studies using *Muc1*$^{-/-}$ mice showed that it forms an important mucosal barrier against *Campylobacter jejuni* infections, a major cause of gastroenteritis.[13] On the contrary, *Muc1*$^{-/-}$ mice exhibited increased mucosal thickness and decreased disease activity index in response to dextran sodium sulfate (DSS) treatment.[14] Spontaneous development of CRC in *Muc2*$^{-/-}$ mice is shown to be due to breach in the inflammatory barrier and *Muc2*$^{-/-}$ mice are more susceptible toward DDS-induced colitis.[11,15] Similarly, a recent study using *Muc13*$^{-/-}$ mice demonstrated that Muc13 is critical in imparting epithelial protection against the cytotoxic agents.[12]

MUC4, a large type-I transmembrane glycoprotein, is normally expressed in the intestinal, reproductive and airway epithelial cells. It is composed of an N-terminal MUC4α subunit that harbors the hallmark tandem repeat domain, nidogen and adhesion-associated MUC4 and other proteins domains, and a C-terminal MUC4β subunit with von Willebrand factor type D, three epidermal growth factor like domains, a transmembrane domain and a short

cytoplasmic tail.[16] Although initially identified as a tracheobronchial mucin from human tracheobronchial mucosal library, it is *de novo* expressed in pancreatic cancer patients imparting tumorigenic and metastatic functions to pancreatic cancer cells.[17] In addition, aberrant expression of MUC4 has been reported in ovarian,[18] breast,[19] lung,[20] gall bladder[21] and biliary tract[22] malignancies. Further, MUC4 is associated with poor clinical outcome in pancreatic ducal adenocarcinoma,[23] intrahepatic chilangiocarcinoma[24] and extrahepatic bile duct carcinoma.[22]

Although MUC4 constitutes an important component of glycocalyx in the intestine, our understanding of its role in intestinal pathologies including inflammatory and neoplastic conditions is limited. Immunohistochemical and/or mRNA expression analyses of UC and CD patient samples resulted in inconclusive findings with some studies suggesting increased or decreased expression, whereas others showing no change in MUC4 expression. However, MUC4 expression was increased in UC patients when associated with neoplastic conditions[8] and in mice treated with DSS to induce acute and chronic colitis.[25] Similarly, few studies have reported the expression pattern of MUC4 during CRC progression suggesting increase, decrease and/or no correlation of MUC4 expression with different stages of CRC.[26–28] However, a recent study by Shanmugam *et al.*[29] showed that early-stage CRC patients with high MUC4 expression exhibit poorer survival compared to those with low MUC4. Besides, no studies have shown any functional role of MUC4 using colon cancer cells. Therefore, to decipher the biological significance of MUC4 in physiological and pathological conditions, we generated *Muc4*$^{-/-}$ mice and explored its role in inflammation-induced colitis and CRC.

RESULTS

Generation and characterization of *Muc4*$^{-/-}$ mice

MUC4, a large type-I transmembrane mucin, is normally expressed by the epithelial cells of small and large intestine. Its murine homolog is encoded by 27 exons and is located on chromosome 16. However, exact role of Muc4 in intestinal pathologies is not known. To understand the biological functions of Muc4, we generated a *Muc4*$^{-/-}$ mouse using a targeting construct obtained from Knockout Mouse Project Repository targeting exons 2–6 (Figure 1a). This is a deletion design that incorporates a splice acceptor and a *LacZ* reporter by replacing the exons 2–6 of *Muc4*. The insertion of the *LacZ* reporter serves two purposes. First, it indicates loss of Muc4. Second, *LacZ* expression indicates the promoter activity of Muc4 in tissues and organs. Mouse embryonic stem cells (129/Sv) electroporated with the targeting construct to obtain the appropriate homologous recombination were validated using long-range PCR (Supplementary Figure 1a) and Southern blot (Supplementary Figure 1b) analyses. Two positive clones micro-injected into C57BL/6J blastocysts were implanted into surrogate females to obtain the chimeras that were backcrossed with C57BL/6J for germ line transmission. Further intercrossing between the F1 progenies was performed to obtain heterozygotes and homozygous *Muc4*$^{-/-}$ animals. All genotypes were determined by PCR using tail DNA (Figure 1b). Reverse transcriptase–PCR analysis confirmed loss of *Muc4* expression in organs that normally express Muc4, that is, colon and lungs (Figure 1c). Pancreas was used as a Muc4 non-expressing organ (Figure 1c) control. With intact Muc4 promoter, a successful deletion of Muc4 would result in LacZ expression in tissues that

normally express Muc4. LacZ staining of different *Muc4*$^{-/-}$ tissues further confirmed the deletion of Muc4 in colon and testes (Figure 1d). Pancreas was used as a non-expressing organ control (Figure 1d). *Muc4*$^{-/-}$ mice are viable, fertile and developed normally with normal sized litters when intercrossed between the heterozygotes. No obvious phenotypic abnormalities were observed in *Muc4*$^{-/-}$ mice up to 1 year of age compared with wild-type (WT) control littermates. To assess whether deletion of Muc4 influences the carbohydrate content in the colon, we performed periodic acid–Schiff and Alcian blue staining that recognize the neutral and acidic carbohydrates, respectively. However, no significant differences in the glycan contents of the colon were observed upon deletion of Muc4 (Supplementary Figure 2).

Muc4$^{-/-}$ mice display increased resistance to DSS-induced colitis Administration of DSS in the drinking water is one of the most widely used and reliable experimental model to induce colonic inflammation.[30] To assess the role of Muc4 in acute colitis, 6- to 8- week-old *Muc4*$^{-/-}$ and WT mice were challenged with 3% DSS in drinking water for 3 weeks and lethality rate was determined. In case of both males (Figure 2a) and females (Figure 2b), *Muc4*$^{-/-}$mice displayed better survival compared with the WT. However, male mice of either group were more susceptible and succumbed earlier compared with females. Therefore, the survival rate was analyzed separately for males and females (Figures 2a and b).

Next, to assess the role of Muc4 in intestinal restitution following tissue injury, 6- to 8-week-old WT and *Muc4*$^{-/-}$ mice were given 2% DSS in drinking water for 7 days followed by 7 days of regular water and were assessed for their body weight, stool consistency and fecal blood every day. We again observed that female mice of either group are more resistant to disease severity compared with males and were analyzed separately. With respect to body weight, increased loss was observed in WT compared with *Muc4*$^{-/-}$ males, however, it was not statistically significant (Figure 2c). In case of females, the body weight loss was not very different (Supplementary Figure 3a) between WT and *Muc4*$^{-/-}$ mice. WT mice exhibited severe diarrhea (Figure 2d) and fecal bleeding (Figure 2e) compared with *Muc4*$^{-/-}$ mice demonstrating that loss of Muc4 imparts increased resistance to DSS-induced colitis. However, no significant difference in diarrhea score was observed between female mice of WT and *Muc4*$^{-/-}$groups (Supplementary Figure 3b) and no rectal bleeding were observed until the end of the experiment. Both male and female WT mice had shortened and edematous colon compared with *Muc4*$^{-/-}$ mice (Figure 2f and Supplementary Figure 3c).

Histologically, WT mice displayed extensive erosion, ulceration, severe crypt damage and massive infiltration of inflammatory cells in to the colonic mucosa compared with *Muc4*$^{-/-}$ mice (treated with 2% DSS in drinking water for 7 days followed by 7 days of regular water) (Figure 3a). The severity and the extent of tissue damage were more pronounced in the distal compared with the proximal colon. As mentioned earlier, the histological score was observed to be statistically significant in male (Figures 3a and b), but not in female mice (Supplementary Figure 3d). Interestingly, an instance of reepithelialization, a process that is prerequisite for restoring normal intestinal mucosal following injury was observed in two *Muc4*$^{-/-}$ mice (Supplementary Figure 4) but not in WT mice (treated with 2% DSS in drinking water for 7 days followed by 7 days of regular water) indicating a rapid healing response in absence of Muc4. Although we observed a discrepancy in the susceptibility of

male and female mice to DSS-induced colitis, our findings in the male animals conclusively demonstrate that the *Muc4*$^{-/-}$ mice displayed increased resistance to DSS-induced colitis compared with their WT counterparts.

Analysis of expression of intestinal mucin genes in WT and *Muc4*$^{-/-}$ mice in response to DSS treatment

To investigate whether deletion of Muc4 results in the compensatory upregulation of any of the colonic mucins and/or expressional variation of colonic mucins in response to DSS treatment (treated with 2% DSS in drinking water for 7 days followed by 7 days of regular water), we analyzed the mRNA expression of *Muc1*, *Muc2*, *Muc3* and *Muc13* in WT and *Muc4*$^{-/-}$ mice with and without DSS treatment. We observed an increase in Muc4 expression in WT mice treated with DSS compared with untreated, however, it was not statistically significant (Figure 4a). Further, under no DSS treatment condition, loss of Muc4 led to significant upregulation of the secretory mucin *Muc2* without any effect on *Muc1*, *Muc3* and *Muc13* (Figure 4b). Following DSS treatment, *Muc3* expression was significantly upregulated and the level of *Muc2* expression was still higher though was not statistically significant (Figure 4c). This demonstrates that Muc4 influences the expression of other intestinal mucins such as *Muc2* and *Muc3* under basal as well as inflammatory conditions. To understand whether loss of Muc4 (MUC4) from the epithelial cells alone elicits compensatory upregulation of mucins such as MUC2 and MUC3, we down-regulated MUC4 in HCT-8 colon cancer cells using two short hairpin RNA oligos (Supplementary Figure 5a). Downregulation of MUC4 in the epithelial cells led to compensatory upregulation of MUC2 (Supplementary Figure 5b) suggesting this may be an epithelial cell intrinsic phenomenon (MUC3 was not expressed in HCT-8 cells).

Reduced infiltration of CD3^{+} T-lymphocytes and F4/80^{+} histiocytes along with reduced expression of inflammatory cytokines in *Muc4*$^{-/-}$ mice following DSS treatment

We assessed the infiltration of inflammatory cells associated with DSS-induced colitis of WT and *Muc4*$^{-/-}$ mice (treated with 2% DSS in drinking water for 7 days followed by 7 days of regular water) by immunohistochemical analysis of colonic tissues using anti-CD3 antibody for T-lymphocytes and anti-F4/80 antibody for histiocytes. Compared with WT mice, *Muc4*$^{-/-}$ mice had significantly reduced histiocytes and T-lymphocytes in the inflamed colonic mucosa (Figures 5a and b). Consequently, mRNA expression analysis of inflammatory cytokines such as tumor necrosis factor (*TNF)-α* showed a significant reduction and a trend in the downregulation of interleukin (*IL)-1β* in the colonic tissues from *Muc4*$^{-/-}$compared with WT mice (Figure 5c). In addition to the inflammatory cytokines, there were significantly lower mRNA levels of anti-microbial enzymes *lysozyme M* and *SLPI* in the colonic mucosa of *Muc4*$^{-/-}$ mice treated with DSS compared with WT mice (Figure 5d).

Muc4$^{-/-}$ mice displayed increased resistance to colitis-associated colorectal tumors in AOM/DSS model

Chronic inflammatory conditions of the colon such as UC and CD are major risk factors for CRC.[31] Having established that Muc4 exacerbates the inflammatory condition of the colon in response to DSS, we investigated the role of Muc4 in colitis-associated CRC using the

well-established azoxymethane (AOM)/DSS model. Twenty-four weeks following administration of AOM/DSS (Figure 6a), WT and *Muc4*$^{-/-}$ mice were analyzed for tumors in the colorectal region. Primarily, the malignant tumors were observed in the distal colon and rectum with occasional small adenomas in the proximal colon. Approximately fourfold higher number of tumor nodules were observed in WT mice compared with *Muc4*$^{-/-}$ mice (Figures 6b and c) and the size of the tumor nodules were larger in WT compared with *Muc4*$^{-/-}$ mice (Figures 6b and c). Histologically, most of the lesions were adenocarcinomas with different degrees of differentiation in both WT and *Muc4*$^{-/-}$ mice. In the *Muc4*$^{-/-}$ group, there was a prevalence of carcinoma *in situ* and low-grade adenocarcinomas with invasion into lamina propria (Figure 7a). Occasional invasion to submucosa was also observed. On the other hand, in WT group there was a prevalence of high-grade adenocarcinomas with frequent invasion into submucosa and occasional invasion into muscularis propria (Figure 7a).

To investigate the molecular mechanism by which loss of Muc4 imparts resistance to colorectal tumorigenesis, we performed immunohistochemical analysis of cellular proliferation (Ki67) and apoptosis (cleaved caspase-3) of the colonic tumors from WT and *Muc4*$^{-/-}$ mice. We observed a significant reduction in the percentage of Ki67-positive cells in the tumors from *Muc4*$^{-/-}$ mice group compared with WT mice (Figures 7b and c) suggesting presence of Muc4 influences the colonic epithelial cell proliferation that was abrogated in *Muc4*$^{-/-}$ mice. There was no difference in the cleaved caspase-3 staining between the WT and *Muc4*$^{-/-}$ mice tumors (data not shown). Altered β-catenin signaling is frequently observed and is the major molecular pathway in human CRC development and progression.[32,33] Immunohisto-chemical analysis of tumors from the WT and *Muc4*$^{-/-}$ mice displayed a strong nuclear β-catenin signal. In both groups cytoplasmic β-catenin signal was present in the adjacent benign mucosa (Figure 7d).

DISCUSSION

IBD that includes UC and CD is a major health problem in the western world.[2] Although the etiology and the mechanism(s) of IBD pathogenesis is multi-factorial and incompletely understood, a dysfunctional mucus barrier on the surface of the luminal epithelial cells is considered to be a major factor.[2] In addition, patients with IBD are at a higher risk of developing CRC.[31] MUC4 is an important component of the glycocalyx on the surface of colonic epithelial cells and is believed to be critical for mucosal protection in addition to other secretory (MUC2) and cell surface mucins (MUC1, MUC3 and MUC13).[3] However, the expression pattern and the role of MUC4 during inflammatory and neoplastic conditions of colon are not well understood. Here, we generated mice that is genetically deficient in Muc4 and addressed the *in vivo* functional relevance of Muc4 during DSS-induced colitis and AOM/DSS-induced CRC. Mice lacking Muc4 were more resistant to colitis and colitis-associated symptoms as well as colitis-associated CRC induced by AOM/DSS. These data demonstrate that Muc4 exacerbates the effects of colitis and colitis-associated CRC.

Upon deletion of Muc4, we did not observe any histological abnormality in the colon of *Muc4*$^{-/-}$ mice compared with WT under steady-state conditions. In addition, the compositions of the neutral and acidic carbohydrates were not significantly altered.

However, the expression of *Muc2* was found to be significantly upregulated in *Muc4*$^{-/-}$ mice compared to WT suggestive of compensatory upregulation. Following DSS treatment, a significant upregulation of *Muc3* (orthologue of human *MUC17*) was observed with *Muc2* expression still on the higher side (although not statistically significant). As *Muc2*$^{-/-}$ mice are prone to spontaneous and DSS-induced colitis,[15] upregulation of *Muc2* in *Muc4*$^{-/-}$ mice could be one of the reasons for increased resistance of *Muc4*$^{-/-}$ mice to DSS-induced colitis. Previous studies using recombinant protein fragments of Muc3/MUC17 and MUC17 knockdown have demonstrated that Muc3/MUC17 has a critical role in maintaining intestinal epithelial barrier to enteroinvasive *Escherichia coli* infection and accelerated healing in response to chemical-induced colitis.[34–36] Therefore, upregulation of *Muc3*, an orthologue of human *MUC17* that helps in intestinal restitution and healing of experimental colitis, in *Muc4*$^{-/-}$ mice treated with DSS also partly explains the resistance displayed by *Muc4*$^{-/-}$ mice to DSS-induced colitis. Accordingly, we observed that the process of reepithelialization that is required for the healing following mucosal injury in *Muc4*$^{-/-}$ mice, but not in WT mice. However, this needs to be validated in a larger cohort to attribute any role of Muc4 in preventing the process of reepithelialization.

Although inflammatory environment is known to influence mucin expression, our study demonstrates that Muc4 also influences the expression of other mucin genes under basal and inflammatory conditions. Particularly, previous studies have demonstrated that proinflammatory cytokines such as TNF-α, IL-1β, IL-4 positively regulate MUC2 expression in human colon cancer and airway epithelial cells.[37–40] Promoter analysis of mouse Muc3 gene revealed binding sites for NF-κB, SP1, CREB and was responsive for the treatment of IL-4, IL-6, TNF-α and so on.[41] As DSS-treated *Muc4*$^{-/-}$ mice show increased expression of proinflammatory cytokines such as TNF-α and IL-1β, these inflammatory mediators may be one of the reasons for upregulation of Muc2 and Muc3 in *Muc4*$^{-/-}$ mice. But, how Muc4 influences the inflammatory environment with and without DSS treatment further needs to be investigated. Further, downregulation of MUC4 in HCT-8 colon cancer cells (epithelial origin) was sufficient to induce compensatory upregulation of *MUC2*, suggesting this compensation may be an epithelial cell intrinsic phenomenon. Therefore, a more holistic approach, including single-cell tran-scriptomics, cytokine array and so on, would be required to further elucidate the exact mechanism of compensatory upregulation of other mucins following deletion of Muc4.

DSS-induced colitis that resembles the phenotypes of UC is one of the most widely used experimental colitis model. It is believed to destabilize the intestinal mucus layer making it more permeable to intestinal luminal content including luminal bacteria.[30] Using the DSS-induced colitis model, we observed a significant resistance toward the severity of colitis as assessed by body weight loss, diarrhea and fecal blood score, extent of tissue damage, and inflammatory cell ($CD3^+$ T-lymphocytes and $F4/80^+$ histiocytes) infiltration in *Muc4*$^{-/-}$ mice compared with WT mice. The inflammatory cytokines such as TNF-α and IL-1β have a critical role in the pathogenesis of IBD[42] and upregulation of these cytokines in WT mice suggests the involvement of Muc4 in IBD pathogenesis. Although the inflammatory cell infiltration and cytokine production could be due to the damage inflicted by DSS, a direct role of Muc4 in immune cell functions cannot be ruled out owing to the resistance displayed by the *Muc4*$^{-/-}$ mice in response to DSS treatment compared with WT mice.

Although Muc4 and Muc13 belong to the transmembrane mucins category, deletion of either of them resulted in opposite phenotypes in response to DSS treatment. Although *Muc13*$^{-/-}$mice resulted in aggressive phenotype (increased loss of body weight, diarrhea score, fecal blood score and severe histologic damage) in response to DSS-induced colitis,[12] *Muc4*$^{-/-}$ mice resulted in protective phenotype (decreased loss of body weight, diarrhea score, fecal blood score and less severe histologic damage). Loss of Muc13 resulted in increased susceptibility of colonic epithelial cells to apoptosis suggesting Muc13 provides protection to colonic epithelial cells from apoptotic stimuli, thereby protecting it from damage-induced cell death. No compensatory upregulation of other mucins such as *Muc1, Muc3* and *Muc4* was observed in *Muc13*$^{-/-}$ mice, whereas compensatory upregulation of *Muc2* and *Muc3* was observed in *Muc4*$^{-/-}$ mice, which we propose as one of the mechanisms by which lack of Muc4 provides protection to colonic epithelial cells. Muc1, another transmembrane mucin, when deleted resulted in protection of colonic epithelial cells[14] like that of *Muc4*$^{-/-}$ mice when challenged with DSS.

As patients with IBD are at greater risk for developing CRC,[31] we addressed the role of Muc4 in WT and *Muc4*$^{-/-}$ mice using a well-established AOM/DSS model. As in DSS-induced colitis model, *Muc4*$^{-/-}$ mice were found to be more resistant to AOM/DSS-induced CRC compared with WT mice. Although several studies have asserted the oncogenic role of MUC4 in multiple malignancies including pancreatic, gastric, breast, ovarian cancer and so on,[17,43–49] the pattern of expression and functional role of MUC4 in colon cancer is not well understood. Few studies investigated the expression pattern of MUC4 during CRC progression suggesting increase, decrease and/or no correlation of MUC4 expression with different stages of CRC.[26–28] A recent study by Shanmugam *et al.*[29] showed that early-stage CRC patients who have high MUC4 expression exhibit poorer survival compared to those with low MUC4. Our study in *Muc4*$^{-/-}$ mice using AOM/DSS model of CRC suggests that Muc4 is involved in the progression of the CRC, where inflammation has a significant role. MUC4 may also be associated with poor prognosis in the subset of IBD patients who develop CRC. However, this needs to be validated in a large cohort of IBD patients that eventually develop CRC. Our future study will aim to address the role of Muc4 in inflammation-independent CRC using genetically defined *CDX2P-NLSCre;Apc*$^{+/loxP}$ and *CDX2P-NLSCre;KRas*$^{G12D/+}$ models of CRC.

We found that WT mice frequently had high-grade adenocarcinomas with deeper in growth into the colonic wall than *Muc4*$^{-/-}$mice. These findings are in agreement with the tumorigenic and metastatic role of MUC4 observed in various other epithelial malignancies.[43,47,48] The Muc4-mediated tumorigenicity may be associated with increased cell proliferation as we found significantly higher Ki67-positive tumor cells in WT group compared with *Muc4*$^{-/-}$ group. Interestingly, there was no apparent difference in the apoptotic activity between the two groups (data not shown). Altered β-catenin signaling is frequently implicated in human CRC development and progression.[32,33] We found that the levels of nuclear β-catenin expression were similar in two groups. It may indicate a common mechanism of colon cancer in these two mouse models. It also suggests certain comparability with human CRC.

Taken together, we demonstrated for the first time *in vivo* relevance of Muc4 in colitis and colitis-associated CRC using mice genetically deficient in Muc4. These *Muc4*$^{-/-}$ mice are highly resistant to chemical-induced colitis and CRC. These mice will further be useful in understanding the role of Muc4 in intestinal infections as well as colitis-independent CRC.

MATERIALS AND METHODS

Generation of *Muc4*$^{-/-}$ mice

The targeting construct for the *Muc4* gene knockout was obtained from the Knock Out Mouse Project Repository (UC Davis). The schematic for the WT and targeted allele are depicted in Figure 1a. The targeting construct included an *IRES-LacZ* cassette in place of exons 2–6 of *Muc4* that gets expressed in tissues and cells wherever *Muc4* promoter is active. The cells positive for a β-galactosidase staining indicates loss of *Muc4*. The targeting construct was electroporated into murine embryonic stem cells (129/SvJ) by homologous recombination. The surviving colonies after G418 selection were screened using long-range PCR and few positive clones were confirmed by Southern blotting (Supplementary Figure 1). Two ES cell clones that had undergone correct homologous recombination were microinjected into C57BL/6J blastocysts, the resultant chimeras were bred to C57BL/6J mice for germ line transmission. Heterozygous F1 progenies were bred to generate homozygous Muc4 KO mice (*Muc4*$^{-/-}$). Genotypes of the mice were determined by PCR using the genomic DNA extracted from the tail. Primers used for genotyping are listed in Supplementary Table-1 (A). Six- to 8-week-old mice in the 129/Sv and C57BL/6J mixed background were used for experiments. WT littermates were used as controls. All mouse experiments were performed in compliance with protocols approved by the Institutional Animal Care and Use Committees of the University of Nebraska Medical Center.

LacZ staining

LacZ staining was performed according to previously published protocol.[50] Briefly, organs collected were washed in phosphate-buffered saline (PBS), fixed for 4 h in lacZ fixative (0.2% glutaraldehyde, 5 mM EGTA and 100 mM $MgCl_2$ in PBS), washed three times in lacZ wash buffer (2 mM $MgCl_2$, 0.01% sodium deoxycholate, and 2.5% NP-40 in PBS), cryoprotected in 15% sucrose/PBS for 1 h at 4 °C followed by 30% sucrose/PBS overnight at 4 °C, and cryosections were prepared. In all, 7-μm thick cryosections of different tissues from the WT and *Muc4*$^{-/-}$ mice were fixed in 0.2% glutaraldehyde for 10 min and then washed with lacZ wash buffer three times. The slides were stained overnight in lacZ stain solution (0.5 mg/ml X-gal, 5 mM potassium ferrocyanide and 5 mM potassium ferricyanide in lacZ wash buffer) at 37 °C. The slides were rinsed in PBS and were stained with nuclear fast red.

Histology and immunohistochemistry

For histology and immunohistological analyses, tissues collected from WT and *Muc4*$^{-/-}$ mice were fixed in 10% buffered formalin, processed, paraffin embedded and sectioned (5 μm). Tissue sections were stained with hematoxylin and eosin (for pathological evaluation), periodic acid–Schiff (Sigma-Aldrich, St Louis, MO, USA; for neutral carbohydrates), Alcian blue (Poly Scientific, Bay Shore, NY, USA; for acidic polysaccharides). For

immunohistochemical analysis using antibodies, sections were deparaffinized in xylene (x4) and then rehydrated with graded alcohols. Endogenous peroxidase was blocked using 3% H_2O_2 in methanol for 30 min. Antigen retrieval was performed using 0.01 M preheated citrate buffer (pH – 6.0, 90 °C) for 15 min. The slides were then washed with PBS and blocked using horse serum (ImmPRESS kit; Vector Labs, Burlingame, CA, USA) for 2 h. The sections were incubated overnight at 4 °C with respective primary antibodies diluted in PBS (anti-CD3, 1:300, Abcam, Cambridge, MA, USA; #ab16669; anti-F4/80, 1:75, e-Biosciences, San Diego, CA, USA; #14-4801-82; anti-β-catenin, 1:500, BD-Biosciences, San Jose, CA, USA; #610153; anti-Ki67, 1:300, Abcam, #ab15580). Slides were washed four times with PBS and incubated with appropriate secondary antibody (peroxidase-labeled anti-mouse/anti-rabbit IgG (ImmPRESS kit, Vector Labs) or anti-rat IgG, Thermo Scientific, Grand Island, NY, USA) for 1 h at room temperature. The slides were washed four times in PBS and were developed using DAB as substrate (DAB substrate kit; Vector Labs). The sections were counterstained with hematoxylin (Vectors Lab) and washed in tap water, dehydrated in increasing grades of alcohol (20–100%) and then with xylene and dried. The slides were mounted in paramount mounting medium (Fisher Scientific, Pittsburg, PA, USA) and photographed using Nikon Eclipse E400 light microscope (Kawasaki, Japan). Quantification of $CD3^+$ T-lymphocytes and $F4/80^+$ histiocytes was performed by counting $CD3^+$ and $F4/80^+$ cells in 10 high-powered fields from each mouse. Percentage of ki67-positive cells was calculated as a ratio of number of $Ki67^+$ nuclei to total number of nuclei per high-powered field with 10 high-powered fields from each mouse.

DSS-induced colitis

To determine the lethality because of DSS, mice aged 6–8 weeks (WT and *Muc4*$^{-/-}$ males and females) were given 3% DSS (40 kDa, TdB Consultancy, Uppsala, Sweden) in drinking water for 21 days. Mice were monitored regularly for mortality. To induce colitis, mice were given 2% DSS in drinking water for 7 days followed by 7 days of regular drinking water and killed for histological analysis. During the course of the experiment, mice were monitored daily for their body weight, stool consistency or diarrhea and presence of gross or occult blood in the rectum or stool according to previously published study.[51] Colon length was measured at the end of the experiment. Tissues were then either fixed in 10% formalin and embedded in paraffin for histopathological analysis or were snap frozen in liquid nitrogen for RNA extraction and subsequent mRNA analyses. Histological scoring for the DSS-induced colitis was carried out in a blinded manner with a combined score for extent of infiltration of inflammatory cells and tissue damage separately for proximal and the distal colon.[51]

AOM/DSS-induced colorectal tumorigenesis in mice

Six- to 8-week-old male and female WT and *Muc4*$^{-/-}$ mice were administered a single intraperitoneal injection of AOM (10 mg/kg body weight; Sigma-Aldrich). One week after injection, mice were fed with 2% DSS (40 kDa, TdB Consultancy) in drinking water for 7 days and were then allowed to recover for 15 days. This cycle was repeated two times followed by regular drinking water till killing. Mice were killed at 24 weeks following AOM injection. The colon was cut open longitudinally and examined for the presence of gross

tumors. Number and size of the tumor nodules were recorded. Tissues were then fixed in 10% formalin and embedded in paraffin for histopathological analysis.

Cell culture and transfections

HCT-8 colon cancer cells from ATCC (Manassas, VA, USA) were cultured in alpha-minimum essential medium supplemented with 10% fetal bovine serum, 100 U/ml penicillin and 100 μg/ml streptomycin and 4 mM L-glutamine. MUC4 was knocked down in HCT-8 cells using two short hairpin RNA oligos (shMUC4 #1: 5′-GGAGATGGCTATTTCGAAA-3′ and shMUC4 #3: 5′-GCATGAAACTCGACGCGTT-3′) cloned into pSUPER.retro. puro vector between *Bgl*II and *Hind*III resctriction sites. Briefly, phoenix cells were transfected with either control (SCR) or short hairpin RNA vectors using Lipofectamine 2000 (Invitrogen, Grand Island, NY, USA) and the supernatants collected at 48 and 72 h following transfection were used to infect HCT-8 cells. After 48 h, cells were grown in medium containing 5 μg/ml of puromycin. The selected pooled populations of cells were used for further experiments.

Immunoblotting

For immunoblotting, cell lysates were collected in RIPA buffer (50 mM Tris-HCl pH-7.5, 150 mM NaCl, 1% NP-40, 0.5% sodium deoxycholate and 0.1% sodium dodecyl sulfate) supplemented with complete protease inhibitor mixture (Roche, New York, NY, USA), 2 mM Na_3VO_4, 10 mM NaF and 1 mM PMSF on ice. Cell lysates cleared by centrifugation were quantified using bicinchoninic acid method and run in 2% sodium dodecyl sulfate–agarose for MUC4 and 10% sodium dodecyl sulfate–polyacrylamide gel electrophoresis for β-actin under reducing conditions and blotted onto polyvinylidene difluoride membrane (Millipore, Massachussets, MA, USA). Membranes were probed with specific antibodies. Blots were washed and probed with respective secondary peroxidase-conjugated antibodies, and the bands visualized by chemiluminescence (Thermo Scientific). Antibodies used were anti-MUC4 (1:1000, 8G7, developed in our lab) and anti-β-actin (1:5000, Sigma, St Louis, MO, USA; #A1978).

RNA extraction from mouse tissues and HCT-8 cells

Tissues collected from the WT and *Muc4*$^{-/-}$ mice were snap frozen in liquid nitrogen and were stored at – 80 °C until further use. Total RNA was extracted using miRVana miRNA isolation kit (Ambion/Life Technologies, Grand Island, NY, USA) according to the manufacturer's instructions. RNA from HCT-8 cells was isolated using RNeasy minikit (Qiagen, Valencia, CA, USA) according to the manufacturer's instructions. The extracted RNA was further treated with DNase I (Qiagen) to obtain pure mRNA without DNA contamination.

Polymerase chain reaction

A total of 2 μg of DNase I-treated mRNA was converted to complementary DNA using either oligo-dT or random hexamer primers and SuperScript reverse transcriptase II (Life Technologies, Grand Island, NY, USA) was used for the reverse transcription according to the manufacturer's instructions. Conventional end point PCR was performed to demonstrate

the loss of Muc4 expression following deletion of Muc4. *Gapdh* was used as an internal reference gene. Primers used for Muc4 expression in conventional PCR are listed in Supplementary Table-1 (B).

Real-time PCR was performed using LightCycler 480 SYBR Green I Master Mix (Roche) with LightCycler 480 II (Roche) Real-Time PCR system. The relative amount of expression was calculated using 2−ΔΔCt method. The average of three independent analyses for each gene and sample was calculated and was normalized to the endogenous reference control gene *Gapdh*. The primers used for expression analysis of mucin genes (*MUC2*, *Muc1*, *Muc2*, *Muc3*, *Muc4* and *Muc13*) and inflammatory cytokines (*IL-1β*, *TNF-α*, *Lysozyme M*, *SLPI* and *IL-10*) are listed in Supplementary Table-1 (C).

Statistical methods

Statistical analyses were carried out using two-tailed Student's *t*-test or Wilcoxon rank sum test and $P \leq 0.05$ was considered to be statistically significant. The Kaplan–Meier method was used to estimate survival distribution and log-rank test was used to compare survival distributions between the groups. SAS software (SAS Institute Inc., Cary, NC, USA) was used for data analysis and R software (R Foundation for Statistical Computing, Vienna, Austria) was used for making box plots. For Kaplan–Meier survival analyses, 15 age-matched animals per group (WT and *Muc4*$^{-/-}$) were randomly distributed and the final analysis was carried out in a blinded manner. For DSS-induced colitis experiment, age-matched 18 WT (males and females combined) and 18 *Muc4*$^{-/-}$ (males and females combined) mice were randomly distributed and all the analyses associated with these animals were performed in a blinded manner. Those animals that died during the course of the experiment were excluded from the analyses. For AOM/DSS-induced CRC experiment, 10 age-matched animals per group (WT and *Muc4*$^{-/-}$) were randomly distributed and the final analysis was carried out in a blinded manner. Animals that died during the course of the experiment were excluded from the analyses. All the animal experiments were performed once and mean values were presented from each group of animals.

Supplementary Material

Refer to Web version on PubMed Central for supplementary material.

Acknowledgments

We thank Don Harms and Rolen Quadros of the mouse genome-engineering core at the University of Nebraska Medical Center (UNMC) for the electroporation, microinjection and generation of chimera for Muc4 knockout mice. We thank UNMC tissue sciences facility for processing of tissues used in the study. We also thank Dr Imayavaramban Lakshmanan and Kavita Mallya for technical assistance. The work in the manuscript, in parts, was supported by the grants from the National Institutes of Health (RO1 CA 78590, RO1 CA183459, UO1CA111294, SPORE P50CA127297, TMEN U54CA163120 and R03 CA167342).

ABBREVIATIONS

AOM	azoxymethane
CD	Crohn's disease

CRC	colorectal cancer
DSS	dextran sodium sulfate
IBD	inflammatory bowel disease
IL	interleukin
TNF	tumor necrosis factor
UC	ulcerative colitis
WT	wild type

References

1. Siegel R, Ma J, Zou Z, Jemal A. Cancer statistics, 2014. CA Cancer J Clin. 2014; 64:9–29. [PubMed: 24399786]
2. Sheng YH, Hasnain SZ, Florin TH, McGuckin MA. Mucins in inflammatory bowel diseases and colorectal cancer. J Gastroenterol Hepatol. 2012; 27:28–38. [PubMed: 21913981]
3. McGuckin MA, Linden SK, Sutton P, Florin TH. Mucin dynamics and enteric pathogens. Nat Rev Microbiol. 2011; 9:265–278. [PubMed: 21407243]
4. Van Klinken BJ, Tytgat KM, Buller HA, Einerhand AW, Dekker J. Biosynthesis of intestinal mucins: MUC1, MUC2, MUC3 and more. Biochem Soc Trans. 1995; 23:814–818. [PubMed: 8654844]
5. Zhang J, Yasin M, Carraway CA, Carraway KL. MUC4 expression and localization in gastrointestinal tract and skin of human embryos. Tissue Cell. 2006; 38:271–275. [PubMed: 16914178]
6. Boltin D, Perets TT, Vilkin A, Niv Y. Mucin function in inflammatory bowel disease: an update. J Clin Gastroenterol. 2013; 47:106–111. [PubMed: 23164684]
7. Longman RJ, Poulsom R, Corfield AP, Warren BF, Wright NA, Thomas MG. Alterations in the composition of the supramucosal defense barrier in relation to disease severity of ulcerative colitis. J Histochem Cytochem. 2006; 54:1335–1348. [PubMed: 16924127]
8. Myerscough N, Warren B, Gough M, Corfield A. Expression of mucin genes in ulcerative colitis. Biochem Soc Trans. 1995; 23:536S. [PubMed: 8654721]
9. Buisine MP, Desreumaux P, Debailleul V, Gambiez L, Geboes K, Ectors N, et al. Abnormalities in mucin gene expression in Crohn's disease. Inflamm Bowel Dis. 1999; 5:24–32. [PubMed: 10028446]
10. Spicer AP, Rowse GJ, Lidner TK, Gendler SJ. Delayed mammary tumor progression in Muc-1 null mice. J Biol Chem. 1995; 270:30093–30101. [PubMed: 8530414]
11. Velcich A, Yang W, Heyer J, Fragale A, Nicholas C, Viani S, et al. Colorectal cancer in mice genetically deficient in the mucin Muc2. Science. 2002; 295:1726–1729. [PubMed: 11872843]
12. Sheng YH, Lourie R, Linden SK, Jeffery PL, Roche D, Tran TV, et al. The MUC13 cell-surface mucin protects against intestinal inflammation by inhibiting epithelial cell apoptosis. Gut. 2011; 60:1661–1670. [PubMed: 21636645]
13. McAuley JL, Linden SK, Png CW, King RM, Pennington HL, Gendler SJ, et al. MUC1 cell surface mucin is a critical element of the mucosal barrier to infection. J Clin Invest. 2007; 117:2313–2324. [PubMed: 17641781]
14. Petersson J, Schreiber O, Hansson GC, Gendler SJ, Velcich A, Lundberg JO, et al. Importance and regulation of the colonic mucus barrier in a mouse model of colitis. Am J Physiol Gastrointest Liver Physiol. 2011; 300:G327–G333. [PubMed: 21109593]
15. Van der Sluis M, De Koning BA, De Bruijn AC, Velcich A, Meijerink JP, Van Goudoever JB, et al. Muc2-deficient mice spontaneously develop colitis, indicating that MUC2 is critical for colonic protection. Gastroenterology. 2006; 131:117–129. [PubMed: 16831596]

16. Chaturvedi P, Singh AP, Batra SK. Structure, evolution, and biology of the MUC4 mucin. FASEB J. 2008; 22:966–981. [PubMed: 18024835]
17. Singh AP, Chaturvedi P, Batra SK. Emerging roles of MUC4 in cancer: a novel target for diagnosis and therapy. Cancer Res. 2007; 67:433–436. [PubMed: 17234748]
18. Chauhan SC, Singh AP, Ruiz F, Johansson SL, Jain M, Smith LM, et al. Aberrant expression of MUC4 in ovarian carcinoma: diagnostic significance alone and in combination with MUC1 and MUC16 (CA125). Mod Pathol. 2006; 19:1386–1394. [PubMed: 16880776]
19. Mukhopadhyay P, Chakraborty S, Ponnusamy MP, Lakshmanan I, Jain M, Batra SK. Mucins in the pathogenesis of breast cancer: implications in diagnosis, prognosis and therapy. Biochim Biophys Acta. 2011; 1815:224–240. [PubMed: 21277939]
20. Majhi PD, Lakshmanan I, Ponnusamy MP, Jain M, Das S, Kaur S, et al. Pathobio-logical implications of MUC4 in non-small-cell lung cancer. J Thorac Oncol. 2013; 8:398–407. [PubMed: 23370366]
21. Miyahara N, Shoda J, Ishige K, Kawamoto T, Ueda T, Taki R, et al. MUC4 interacts with ErbB2 in human gallbladder carcinoma: potential pathobiological implications. Eur J Cancer. 2008; 44:1048–1056. [PubMed: 18397823]
22. Tamada S, Shibahara H, Higashi M, Goto M, Batra SK, Imai K, et al. MUC4 is a novel prognostic factor of extrahepatic bile duct carcinoma. Clin Cancer Res. 2006; 12:4257–4264. [PubMed: 16857800]
23. Saitou M, Goto M, Horinouchi M, Tamada S, Nagata K, Hamada T, et al. MUC4 expression is a novel prognostic factor in patients with invasive ductal carcinoma of the pancreas. J Clin Pathol. 2005; 58:845–852. [PubMed: 16049287]
24. Shibahara H, Tamada S, Higashi M, Goto M, Batra SK, Hollingsworth MA, et al. MUC4 is a novel prognostic factor of intrahepatic cholangiocarcinoma-mass forming type. Hepatology. 2004; 39:220–229. [PubMed: 14752841]
25. Hoebler C, Gaudier E, De Coppet P, Rival M, Cherbut C. MUC genes are differently expressed during onset and maintenance of inflammation in dextran sodium sulfate-treated mice. Dig Dis Sci. 2006; 51:381–389. [PubMed: 16534686]
26. Biemer-Huttmann AE, Walsh MD, McGuckin MA, Ajioka Y, Watanabe H, Leggett BA, et al. Immunohistochemical staining patterns of MUC1, MUC2, MUC4, and MUC5AC mucins in hyperplastic polyps, serrated adenomas, and traditional adenomas of the colorectum. J Histochem Cytochem. 1999; 47:1039–1048. [PubMed: 10424888]
27. Biemer-Huttmann AE, Walsh MD, McGuckin MA, Simms LA, Young J, Leggett BA, et al. Mucin core protein expression in colorectal cancers with high levels of microsatellite instability indicates a novel pathway of morphogenesis. Clin Cancer Res. 2000; 6:1909–1916. [PubMed: 10815915]
28. Ogata S, Uehara H, Chen A, Itzkowitz SH. Mucin gene expression in colonic tissues and cell lines. Cancer Res. 1992; 52:5971–5978. [PubMed: 1394223]
29. Shanmugam C, Jhala NC, Katkoori VR, Wan W, Meleth S, Grizzle WE, et al. Prognostic value of mucin 4 expression in colorectal adenocarcinomas. Cancer. 2010; 116:3577–3586. [PubMed: 20564074]
30. Perse M, Cerar A. Dextran sodium sulphate colitis mouse model: traps and tricks. J Biomed Biotechnol. 2012; 2012:718617. [PubMed: 22665990]
31. Feagins LA, Souza RF, Spechler SJ. Carcinogenesis in IBD: potential targets for the prevention of colorectal cancer. Nat Rev Gastroenterol Hepatol. 2009; 6:297–305. [PubMed: 19404270]
32. Bienz M, Clevers H. Linking colorectal cancer to Wnt signaling. Cell. 2000; 103:311–320. [PubMed: 11057903]
33. MacDonald BT, Tamai K, He X. Wnt/beta-catenin signaling: components, mechanisms, and diseases. Dev Cell. 2009; 17:9–26. [PubMed: 19619488]
34. Luu Y, Junker W, Rachagani S, Das S, Batra SK, Heinrikson RL, et al. Human intestinal MUC17 mucin augments intestinal cell restitution and enhances healing of experimental colitis. Int J Biochem Cell Biol. 2010; 42:996–1006. [PubMed: 20211273]
35. Resta-Lenert S, Das S, Batra SK, Ho SB. Muc17 protects intestinal epithelial cells from enteroinvasive E. coli infection by promoting epithelial barrier integrity. Am J Physiol Gastrointest Liver Physiol. 2011; 300:G1144–G1155. [PubMed: 21393431]

36. Ho SB, Luu Y, Shekels LL, Batra SK, Kandarian B, Evans DB, et al. Activity of recombinant cysteine-rich domain proteins derived from the membrane-bound MUC17/Muc3 family mucins. Biochim Biophys Acta. 2010; 1800:629–638. [PubMed: 20332014]
37. Dharmani P, Leung P, Chadee K. Tumor necrosis factor-alpha and Muc2 mucin play major roles in disease onset and progression in dextran sodium sulphate-induced colitis. PLoS One. 2011; 6:e25058. [PubMed: 21949848]
38. Enss ML, Cornberg M, Wagner S, Gebert A, Henrichs M, Eisenblatter R, et al. Proinflammatory cytokines trigger MUC gene expression and mucin release in the intestinal cancer cell line LS180. Inflamm Res. 2000; 49:162–169. [PubMed: 10858016]
39. Iwashita J, Sato Y, Sugaya H, Takahashi N, Sasaki H, Abe T. mRNA of MUC2 is stimulated by IL-4, IL-13 or TNF-alpha through a mitogen-activated protein kinase pathway in human colon cancer cells. Immunol Cell Biol. 2003; 81:275–282. [PubMed: 12848848]
40. Kim YD, Jeon JY, Woo HJ, Lee JC, Chung JH, Song SY, et al. Interleukin-1beta induces MUC2 gene expression and mucin secretion via activation of PKC-MEK/ERK, and PI3K in human airway epithelial cells. J Korean Med Sci. 2002; 17:765–771. [PubMed: 12482999]
41. Shekels LL, Ho SB. Characterization of the mouse Muc3 membrane bound intestinal mucin 5′ coding and promoter regions: regulation by inflammatory cytokines. Biochim Biophys Acta. 2003; 1627:90–100. [PubMed: 12818427]
42. Bouma G, Strober W. The immunological and genetic basis of inflammatory bowel disease. Nat Rev Immunol. 2003; 3:521–533. [PubMed: 12876555]
43. Singh AP, Moniaux N, Chauhan SC, Meza JL, Batra SK. Inhibition of MUC4 expression suppresses pancreatic tumor cell growth and metastasis. Cancer Res. 2004; 64:622–630. [PubMed: 14744777]
44. Singh AP, Senapati S, Ponnusamy MP, Jain M, Lele SM, Davis JS, et al. Clinical potential of mucins in diagnosis, prognosis, and therapy of ovarian cancer. Lancet Oncol. 2008; 9:1076–1085. [PubMed: 19012856]
45. Singh PK, Hollingsworth MA. Cell surface-associated mucins in signal transduction. Trends Cell Biol. 2006; 16:467–476. [PubMed: 16904320]
46. Senapati S, Das S, Batra SK. Mucin-interacting proteins: from function to therapeutics. Trends Biochem Sci. 2010; 35:236–245. [PubMed: 19913432]
47. Senapati S, Chaturvedi P, Sharma P, Venkatraman G, Meza JL, El-Rifai W, et al. Deregulation of MUC4 in gastric adenocarcinoma: potential pathobiological implication in poorly differentiated non-signet ring cell type gastric cancer. Br J Cancer. 2008; 99:949–956. [PubMed: 18781152]
48. Ponnusamy MP, Lakshmanan I, Jain M, Das S, Chakraborty S, Dey P, et al. MUC4 mucin-induced epithelial to mesenchymal transition: a novel mechanism for metastasis of human ovarian cancer cells. Oncogene. 2010; 29:5741–5754. [PubMed: 20697346]
49. Ponnusamy MP, Seshacharyulu P, Vaz A, Dey P, Batra SK. MUC4 stabilizes HER2 expression and maintains the cancer stem cell population in ovarian cancer cells. J Ovarian Res. 2011; 4 7-2215-4-7.
50. Lobe CG, Koop KE, Kreppner W, Lomeli H, Gertsenstein M, Nagy A. Z/AP, a double reporter for cre-mediated recombination. Dev Biol. 1999; 208:281–292. [PubMed: 10191045]
51. Araki A, Kanai T, Ishikura T, Makita S, Uraushihara K, Iiyama R, et al. MyD88-deficient mice develop severe intestinal inflammation in dextran sodium sulfate colitis. J Gastroenterol. 2005; 40:16–23. [PubMed: 15692785]

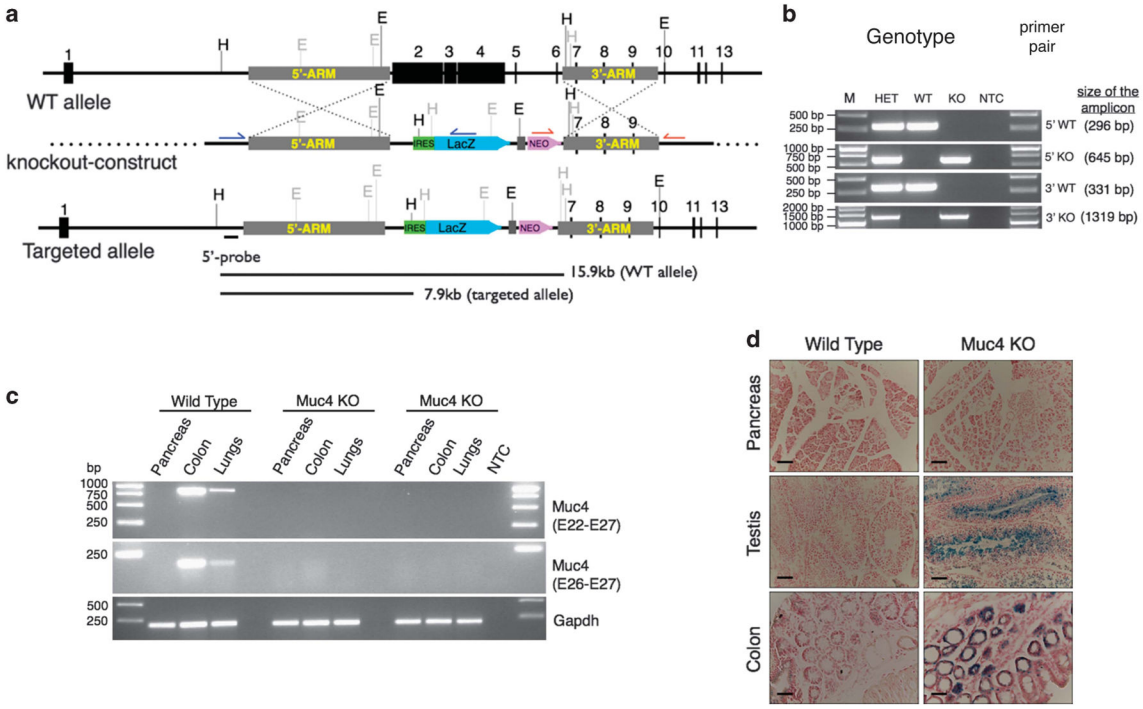

Figure 1.

Targeted disruption of mouse *Muc4* gene. (**a**) Schematic representation of the targeting construct used for generation of *Muc4*$^{-/-}$ mice. The targeting construct containing IRES-LacZ-hbactP-Neo cassette was used to replace exons 2–6 of *Muc4* (represented as the black boxes) through homologous recombination. The blue (⇀) and red (⇀) half arrows indicate the position of the primers used for long-range PCR analysis for homologous recombination at 5′ and 3′ regions respectively. (**b**) PCR analysis using the genomic DNA extracted from the tail biopsies for genotyping. Each mouse was genotyped for WT and KO primer pairs for both 5′ and 3′ regions. (**c**) Reverse transcriptase (RT)–PCR analysis using primers for the 3′ region (exon-22 forward-primer: exon-27 reverse-primer and exon-26 forward-primer: exon-27 reverse-primer) of *Muc4* confirmed the deletion of Muc4. Normal colon and lungs express Muc4, whereas normal pancreas does not. (**d**) LacZ staining of pancreas, testes and lungs from WT and *Muc4*$^{-/-}$ mice. LacZ expression indicates successful deletion of Muc4. As normal pancreas does not express Muc4, LacZ expression is not seen in *Muc4*$^{-/-}$pancreas. Scale bar, 500 μm.

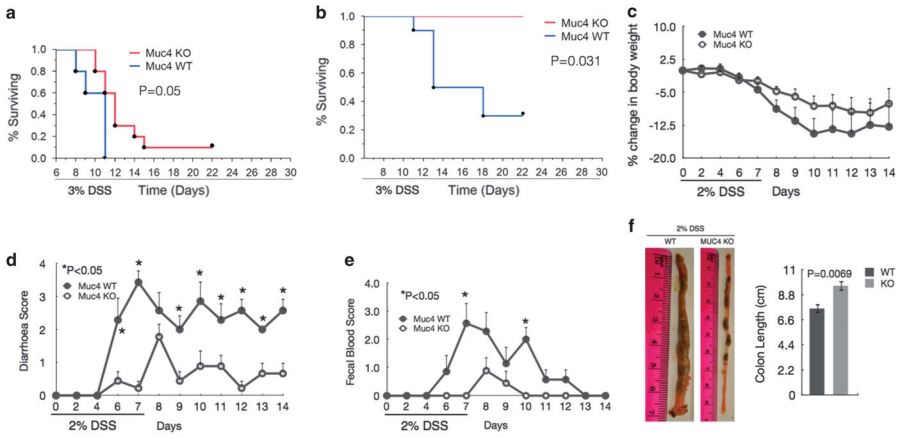

Figure 2.

Muc4$^{-/-}$ mice display enhanced resistance to DSS-induced colitis compared with WT mice. (**a**, **b**) Kaplan–Meier survival analysis of age-matched WT (5 males and 10 females) and *Muc4*$^{-/-}$ (10 males and 5 females) mice following treatment of 3% DSS in drinking water for 21 days; males (**a**) and females (**b**). As female mice of both WT and *Muc4*$^{-/-}$ categories displayed less susceptibility to colitis-induced mortality compared with male mice of either group, we performed separate analysis for males and females using log-rank test (*P*-values shown). (**c**–**e**) Percentage change in body weight compared with the baseline weight (**c**), diarrhea score (**d**) and fecal blood score (**e**) in age-matched WT ($n = 7$) and *Muc4*$^{-/-}$ ($n = 9$) male mice after 2% DSS treatment for 7 days followed by 7 days of regular water. Student's *t*-test; error bars indicate mean ±s.e.m., *P*-values shown. (**f**) WT male mice ($n = 7$) had shortened and edematous colon compared with *Muc4*$^{-/-}$ male mice ($n = 7$) after 2% DSS treatment for 7 days. Student's *t*-test; error bars indicate mean ±s.e.m., *P*-values shown.

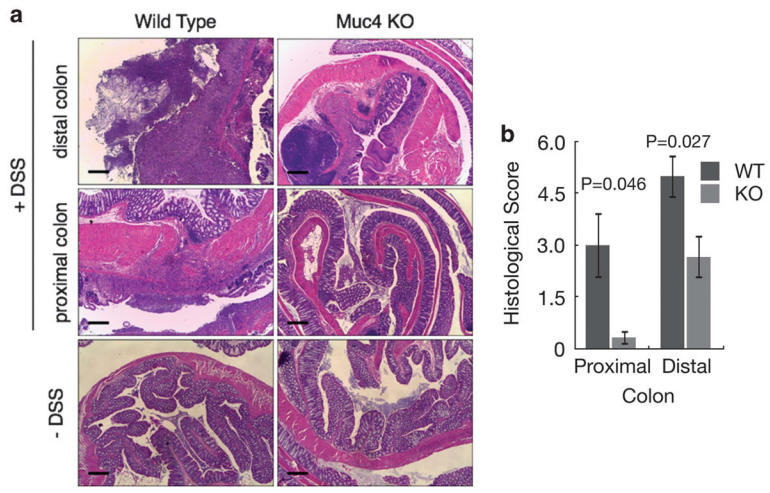

Figure 3.

WT mice exhibit severe histopathological alterations compared with *Muc4*$^{-/-}$ mice following DSS-induced colitis. (**a**) Representative hematoxylin and eosin-stained colonic sections from WT and *Muc4*$^{-/-}$ mice with or without 2% DSS treatment. Although no histological difference was observed in mice without DSS treatment, WT mice displayed extensive epithelial ulceration, erosions, severe crypt damage and massive infiltration of inflammatory cells in to the colonic mucosa compared with the *Muc4*$^{-/-}$ mice. This effect was more pronounced in the distal colon compared with the proximal colon. Scale bar, 500 μm. (**b**) Quantification of histolopathological abnormalities in male WT ($n = 7$) and *Muc4*$^{-/-}$ ($n = 9$) mice following 2% DSS-induced colitis based on extent of tissue damage and inflammatory cell infiltration. Student's *t*-test; error bars indicate mean ±s.e.m., *P*-values shown.

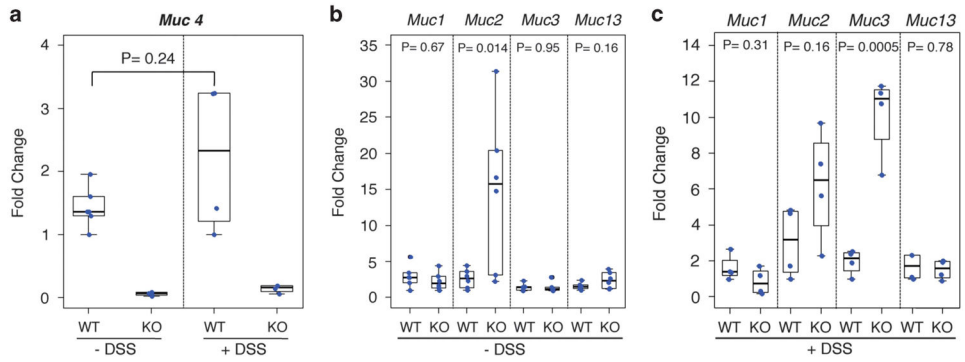

Figure 4.

Expression of colonic mucin genes in WT and *Muc4*$^{-/-}$ male mice in response to DSS-induced tissue damage. (**a**) Expression analysis of *Muc4* was determined using mRNA extracted from the frozen colon tissues from WT and *Muc4*$^{-/-}$male mice with (n = 4) and without (n = 6) 2% DSS treatment. (**b**, **c**) Expression analysis of other colonic mucins *Muc1*, *Muc2*, *Muc3* and *Muc13* was determined using mRNA extracted from the frozen colon tissues from WT and *Muc4*$^{-/-}$ male mice without (n = 6) (**b**) and with (n = 4) (**c**) 2% DSS treatment. Real-time PCR was performed to quantitate the mRNA expression. Expressed relative to *Gapdh* and the fold change in expression was calculated with respect to WT mice. The statistical analysis was done with data transformed to the log2 scale using t-tests, and the means and 95% confidence intervals (CIs) were back transformed to the original scale, P-values shown.

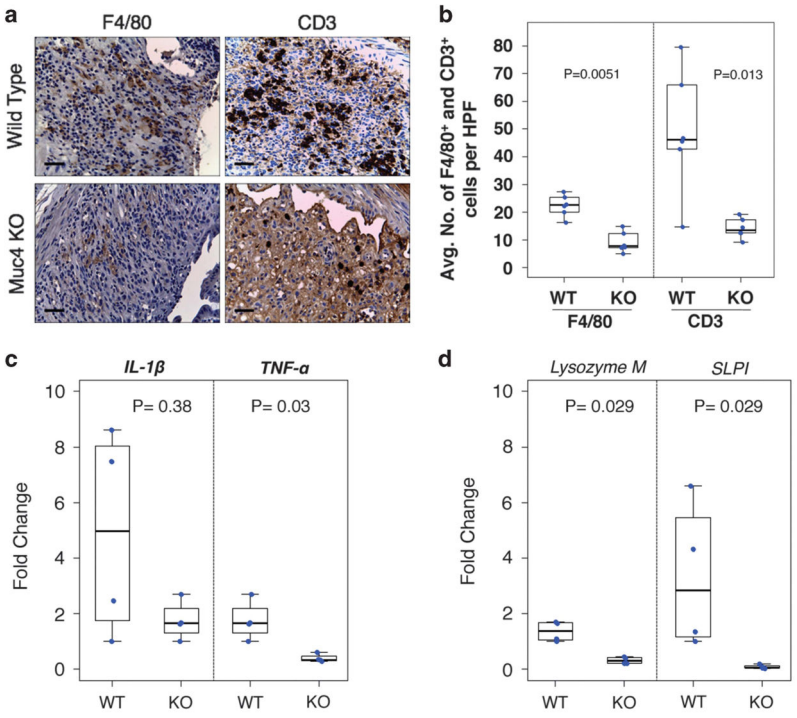

Figure 5.

Reduced infiltration of histiocytes and T-lymphocytes and expression of inflammatory cytokines in the colon of *Muc4*$^{-/-}$ male mice compared with WT male mice following DSS-induced colitis. (**a**) Representative colon sections from WT and *Muc4*$^{-/-}$ male mice stained with F4/80^{+} histiocytes and CD3^{+} T-lymphocytes after 2% DSS treatment for 7 days followed by 7 days of recovery. Scale bar, 500 μm. (**b**) Quantitative representation of average number of F4/80^{+} histiocytes and CD3^{+} T-lymphocytes per high-powered field (HPF) with 10 HPFs per mouse from male WT ($n = 6$) and male *Muc4*$^{-/-}$ mice ($n = 6$). Wilcoxon rank sum test was used to compare the average number of CD3^{+} and F4/80^{+} cells between WT and *Muc4*$^{-/-}$ mice groups, *P*-values shown. (**c**, **d**) Expression analysis of inflammatory cytokines (**c**) and antimicrobial factors (**d**) was determined using mRNA extracted from the frozen colon tissues from WT and *Muc4*$^{-/-}$ male mice with 2% DSS treatment. Real-time PCR was performed to quantitate the mRNA expression ($n = 4$). Expressed relative to *Gapdh* and the fold change in expression was calculated with respect to WT mice. The statistical analysis was done with data transformed to the log2 scale using *t*-tests, and the means and 95% confidence intervals (CIs) were back transformed to the original scale, *P*-values shown.

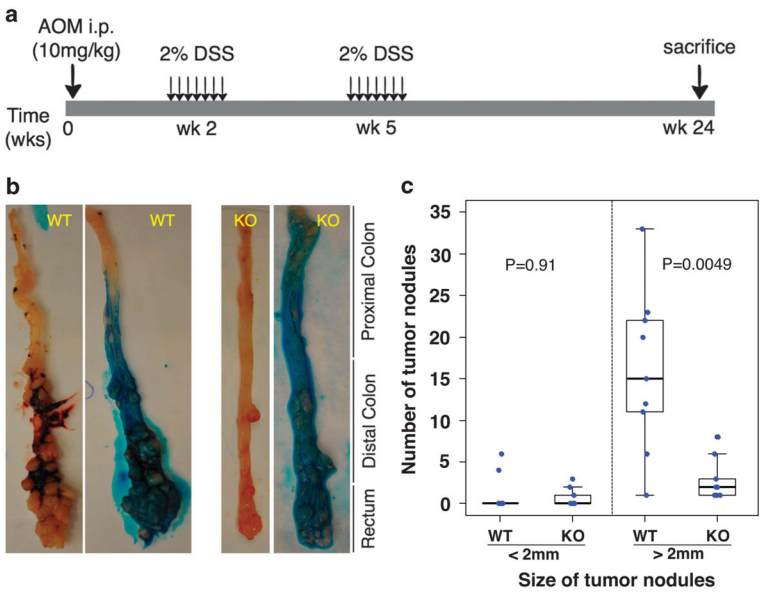

Figure 6.

Colorectal tumorigenesis was delayed and less severe in *Muc4*$^{-/-}$ mice after AOM/DSS treatment. (**a**) Schematic for AOM/DSS treatment protocol for induction of colorectal tumor in WT and *Muc4*$^{-/-}$ mice (both males and females). (**b**) Representative longitudinal luminal views of colons from WT and *Muc4*$^{-/-}$ mice at the end of the AOM/DSS treatment protocol. WT mice display increased number and larger tumor nodules compared with the *Muc4*$^{-/-}$ mice. We used Alcian blue (the blue colored dye) as a smear to demarcate the boundaries of the tumor nodules that was very helpful in counting and measuring the numbers and size of the tumor nodules respectively. (**c**) Tumor nodules were compared between WT ($n = 9$) and *Muc4*$^{-/-}$ mice ($n = 9$), for <2 mm and >2 mm separately using Wilcoxon rank sum test, *P*-values shown. Both male and female mice were included in this study.

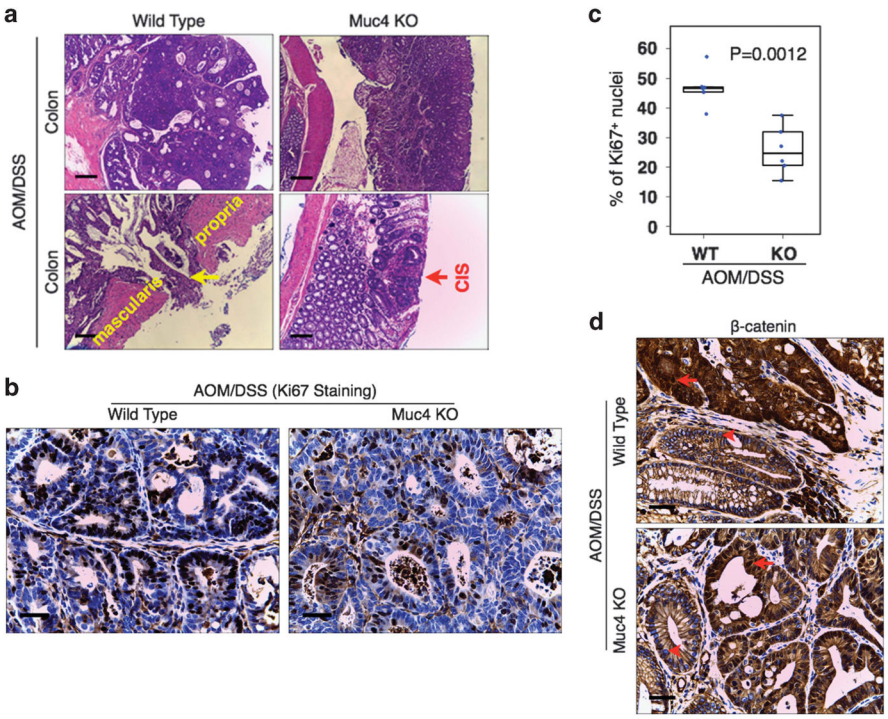

Figure 7.

Muc4-mediated cellular proliferation contributes to enhanced colitis-associated tumorigenesis. (**a**) Representative hematoxylin and eosin-stained colonic sections from the WT and *Muc4*$^{-/-}$ mice after AOM/DSS treatment. Tumors in the WT mice were found with frequent invasion into submucosa and sometimes to muscularis propria (yellow arrow), whereas tumors in the *Muc4*$^{-/-}$ mice were of carcinoma *in situ* (CIS, red arrow) type with invasion into lamina propria. Scale bars, 500 μm. (**b**) Representative colon tumor sections from WT and *Muc4*$^{-/-}$ mice with Ki67 staining. Scale bars, 500 μm. (**c**) Percentage of Ki67^{+} nuclei was determined as a ratio of Ki67^{+} nuclei to total nuclei per high-powered field (HPF) with 10 HPFs per mouse from the WT ($n = 6$) and *Muc4*$^{-/-}$ mice ($n = 7$) group. Wilcoxon rank sum test was used to calculate the statistical significance, *P*-value shown. Both male and female mice were included in this study. (**d**) Representative immunohistochemical staining of colon tumor sections from WT and *Muc4*$^{-/-}$ mice with β-catenin staining. Nuclear β-catenin staining is seen in the neoplastic tissues (red arrow) with the cytoplasmic β-catenin staining in the adjacent non-neoplastic crypts (red arrow heads). Scale bars, 500 μm.